LANSCE 1L HARP DATA ACQUISITION SYSTEM UPGRADE: FIRST RESULTS*

J. Sedillo, D. Martinez, J. Nguyen, LANL, Los Alamos, NM 87545 USA

Abstract

Efforts applied toward the upgrade of the LANSCE 1L harp beam diagnostic data acquisition system have completed with the system's successful deployment in late December 2014. Leveraging the principle of secondary electron emission, the data acquisition system measures the particle beam-induced, negative charge-loss response of a statically-located, harp-style, beam diagnostic sensor. The harp's sense wires span two orthogonal planes, transversely oriented with the beam's direction of travel resulting in two orthogonal profiles. The profile data provided by this beam diagnostic system allows LANSCE operators to measure the particle beam's transverse properties prior to reaching its final destination: the 1L target. Details will be provided with respect to the system's final hardware architecture, the system's theoretical beam response model, and the system's measured beam response.

INTRODUCTION

Shown in Fig. 1, the 1L harp is a fixed-position beam diagnostic sensor for measurement of the beam's transverse profiles immediately prior to impingement on the 1L target. The sensor is composed of three planes of silicon-carbide (SiC) fibers; two sense planes for measuring horizontal and vertical beam profiles, and a bias plane for absorption of secondary electrons. Each sense plane is composed of seventeen sense fibers spaced at 6 mm intervals. All fibers connect to individual 10 pF capacitors at one end and a cable plant at the other end for signal transmission to the data acquisition system [1].

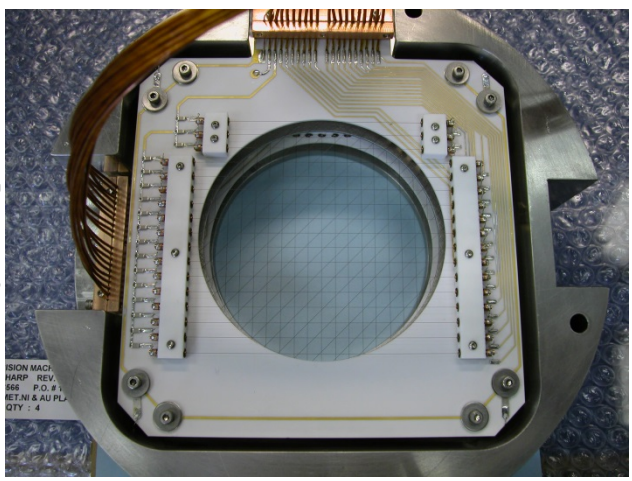

Figure1: 1L harp sensor.

*Funded under the auspices of the US Department of Energy. Contract DE-AC52-06NA25396.

PRINCIPLE OF OPERATION

The 1L harp operates on the principle of secondary electron emission resulting from the interaction of the particle beam with the harp's sense fibers. As the high-energy (800 MeV) H+ particle beam passes through the fiber, electrons from the material are forcefully removed from the fiber's surface into free space, leaving a positive charge gain within the fiber. The positive voltage resulting from the fiber's loss of electrons attracts a flow of electron current from the signal conditioning circuit to the fiber, neutralizing the charge difference. This current and its associated net charge are transformed by the signal conditioning circuitry into a voltage signal proportionally related to the charge. Since the particle beam's transverse particle density is generally Gaussian, each fiber in the plane receives a different amount of beam flux. This beam flux translates into secondary electron emission differences resulting in charge differences at the signal conditioning circuitry and finally a voltage difference at the analog-to-digital converter (ADC) dedicated to each fiber. Plotting the resulting voltages as a function of the fiber's relative position creates a Gaussian profile corresponding to the beam's transverse particle density. General beam and 1L harp parameters are listed in Table 1.

Table 1: 1L Harp and Beam Properties

Beam Property	Value
Beam species	H+
Beam energy	800 MeV
Longitudinal current profile	Triangular
Pulse duration	300 ns
Peak current	33.3 A
Bunch charge	5 μCoulombs
Beam Transverse σ	12.5 mm
Sensor Material	Silicon-Carbide Fiber (SiC)
Sensor Diameter	0.079 mm

BEAM RESPONSE MODEL

In order to model the particle beam's electrical effect on the fibers, the following mathematical tools and theories were employed:

- The Bethe-Bloch stopping power formula [2].

ISBN 978-3-95450-176-2

- Error function for Gaussian integral calculation.
- Sternglass secondary emission yield formula.
- TI ACF2101 electrical response model.

Beam Energy Loss in Silicon-Carbide

The Bethe-Bloch formula describes a beam particle's rate of energy loss per unit distance as it travels through a stopping medium. The formula employed is shown in equation 1. While the stopping material and beam properties required for this calculation are listed in Table 2.

$$-\frac{dE}{dx} = 4\pi N_A r_e^2 m_e c^2 \rho \frac{Zq^2}{A\beta^2}\left[\ln\left(\frac{W_{\max}}{I} - \beta^2\right)\right] \quad (1)$$

$$W_{\max} = 2m_e c^2(\gamma\beta)^2 \quad (2)$$

Table 2: Bethe-Bloch Parameters for the 1L Harp

Parameter	Value
N_A	6.02×10^{23}
r_e, electron radius	2.818×10^{-13} cm
$m_e c^2$, electron rest energy	0.511 MeV
ρ, density of SiC	$3.21 \frac{\text{g}}{\text{cm}^3}$
Z, combined atomic number of Si and C	20
q, charge of a proton	+1
A, combined atomic mass of Si and C	40.1
β, beam velocity ratio relative to speed of light	0.84
γ, beam Lorentz factor	1.85
E_{beam}, beam energy	800 MeV
$m_o c^2$, proton rest mass	938 MeV
W_{max}, maximum energy transfer	2.49
I, ionization potential of SiC [3]	180×10^{-6} MeV

Combining the parameters of Table 2 with equation 1 results in an expected beam energy loss rate or $-\frac{dE}{dx}$ of 6.12 MeV/cm as it travels through a silicon-carbide fiber.

Beam Flux Through a Harp Fiber

A particle beam with a Gaussian, transverse particle/charge density, ideally centered on a thin fiber will provide the maximum amount of particle flux through that fiber. Calculating the particle charge intercepted by the fiber is accomplished by evaluating equation 3, where the Gaussian charge density function is evaluated over the diameter of the wire with a beam of assumed mean position of $\mu = 0$ [5].

$$Q_{i,ratio}(r,\sigma) = \int_{-r}^{r} \frac{1}{\sigma\sqrt{2\pi}} e^{\left(\frac{-x^2}{2\sigma^2}\right)} dx = erf\left(\frac{r}{\sigma\sqrt{2}}\right) \quad (3)$$

Evaluating equation 3 with the relevant parameters of Table 1 (i.e. $r = \frac{0.079}{2}, \sigma = 12.5$) results in $Q_{i,ratio} = 0.0025$, or approximately 0.25% of the beam will be intercepted by a fiber placed at beam center. With a bunch charge of 5 micro-coulombs, a 0.25% flux translates to an intercepted charge of 12.6 nano-coulombs.

Since the beam passes through the fiber with relatively low energy loss, the particle flux is enhanced by the particles emerging from the downstream-side of the fiber. Furthermore, since the fiber has a circular cross-section, a geometrical flux-enhancing feature should be considered. This is accomplished by multiplying the charge flux obtained by π since the flux encounters the entire perimeter of the circular fiber. Accounting for this results in an "effective" intercepted charge of 39.6 nano-coulombs.

Secondary Electron Yield Ratio

Knowledge of the stopping power allows for the calculation of the secondary electron yield, Y, per incident beam particle. A formula that models this phenomenon is defined by equation 4 and is known as the Sternglass Theory [4].

$$Y = \frac{Pd_s}{E^*}\frac{dE}{dx} \quad (4)$$

Table 3 lists the parameters and values suggested by Sternglass along with the energy loss value calculated earlier.

Table 3: Sternglass Parameters for 1L Harp

Parameter	Value
P, probability of electron escape	0.5
d_s, average electron depth	1 nm
E^*, average kinetic energy lost by incident beam particles	25 eV
$\frac{dE}{dx}$, Bethe-Bloch result	6.12 MeV/cm

ISBN 978-3-95450-176-2

Combining the parameters in table 3 with equation 4 results in a yield ratio, Y, of 0.0122 electrons per incident proton.

Knowledge of the effective charge and the yield ratio leads to the determination of charge loss due to secondary emission. Multiplying the effective intercepted charge (39.6 nano-coulombs) by the yield ratio Y (0.0122) results in a maximum expected negative charge loss of 484 pico-coulombs.

ACF2101 Integrator Response

With the expected charge loss determined, it now becomes possible to determine the response of the integrator circuitry. The integrator utilized in the 1L Harp is the Texas Instruments (TI) ACF2101 chip. The integrator circuits of this chip have the behavioral model described by equation 5 [6].

$$V_{out}(t) = \frac{-1}{100 \times 10^{-12}} \int_0^t I(\tau) d\tau = \frac{-Q(t)}{100 \times 10^{-12}} \qquad (5)$$

Substituting the 484 pico-coulomb value into equation 5 results in an integrated response of -4.84 volts. The outputs of the integrators are then digitized by the system's ADCs and negated to positive values prior to profile assembly.

SYSTEM HARDWARE

Beam Signal Conditioning Subsystem/Analog Front End (AFE)

Each ACF2101 integrated circuit features dual, independent integrators with on-die capacitors and multiplexing circuitry for integration, select, reset, and hold operations. Set at 100 pF, the on-die capacitor is capable of measuring up to 1 nano-coulomb of positive charge before the integrator saturates [6]. Beam integration time is variable and can be set by the control logic signals applied to the ACF2101. Additionally, the state of integration is reset after the measurement has been made to prevent interference to subsequent pulse

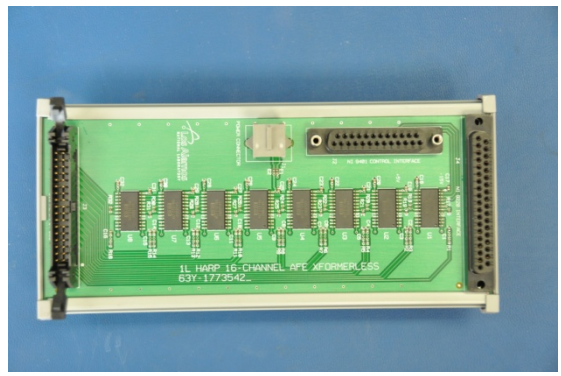

Figure 2: 16-Channel AFE.

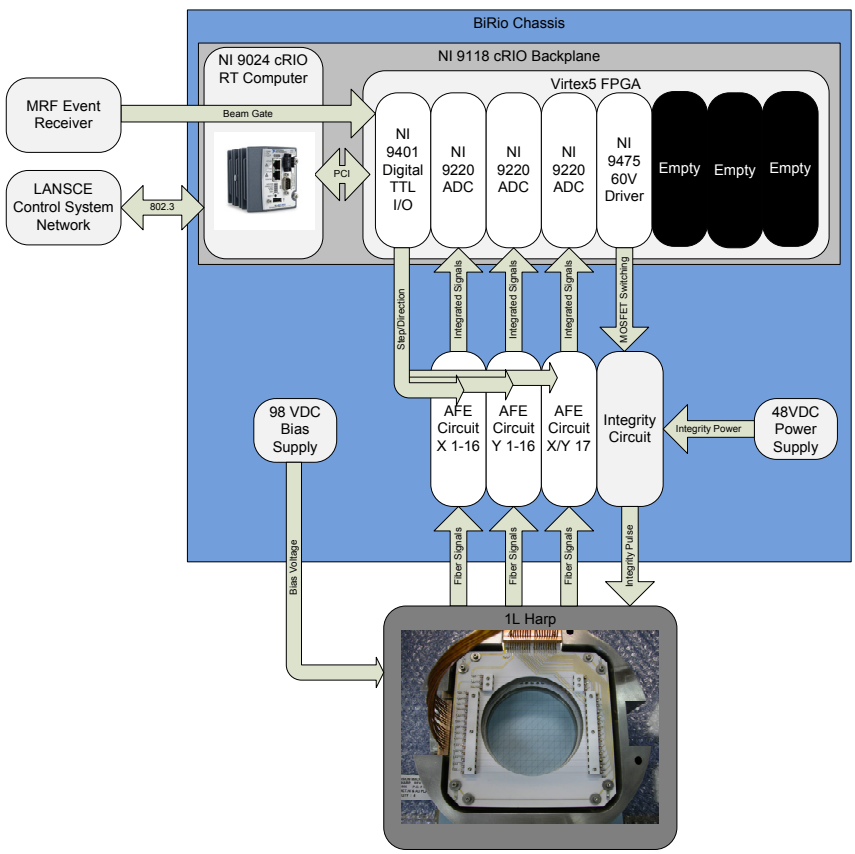

Figure 3: 1L Harp data acquisition system hardware diagram.

ISBN 978-3-95450-176-2

measurements. The final value of each signal's integration is applied to the beam profile for observation. Figure 2 shows one of the system's three AFE circuits. Each board contains eight ACF2101 integrators for processing sixteen channels. Connections to the AFE board include the Harp sensor interface shown on the left of the board, a power connector shown on the top-center, a control connection to the right of the power connector, and the output connector to the ADC on the right.

Data Acquisition System/ EPICS IOC

The overall data acquisition hardware unit (Fig. 3) is composed of a National Instruments CompactRIO computer system with interfaces to the three AFE boards and one integrity board housed within a rack-mountable BiRIO chassis. Logic signals for beam synchronization and ACF2101 control interface to the compactRIO through one NI-9401 10 MHz, 5V TTL logic module. Signals generated by the ACF2101's are digitized by three NI-9220 16-channel, 100kHz, +/-10V ADC modules. Finally, one NI-9475 60V-source module is incorporated for integrity pulse generation. Additional circuitry includes a 100V power supply for the harp bias plane.

Integrity Subsystem

As beam-induced sensor damage is a common mode of failure with harp diagnostics, a fiber integrity subsystem has been incorporated for monitoring the continuity of the fibers. This is accomplished by sending a 48 volt, square pulse to the 10 pF capacitor-end of the fibers. The 10 pF capacitors are applied in series to each wire at the harp and function to AC-couple the 48 volt pulse to the fiber. As the pulse translates through the capacitor-fiber circuit, it is attenuated to a signal on the order of 20 mV with an expected charge displacement of 480 pico-coulombs. Measurement of this signal occurs in the same manner as the beam signal; via charge integration. Through this method, an acceptable integrity signal can be read as -4.8 Volts by the ADCs.

SYSTEM SOFTWARE

FPGA Software Architecture

Harp data acquisition starts with the compactRIO's FPGA and its associated I/O modules. The FPGA program consists of two parallel operations (Fig. 4). The first of these simultaneously monitors the beam synchronization/gate pulse and applies the control signals for all ACF2101 integrators via the NI-9401 module. Since the gate pulse has a narrow, 300 ns pulse width, the NI-9401 must sample at its fastest operating rate of 10 MHz to achieve 2-3 samples per pulse. When the gate has been detected by this process, an internal flag is set, signalling the second parallel process. The primary purpose of the second process is to continuously sample the wire signals at the maximum ADC sampling rate. Once notified of a gate, this process will save the set number (typically 2) of pre-gate, rising-edge samples and

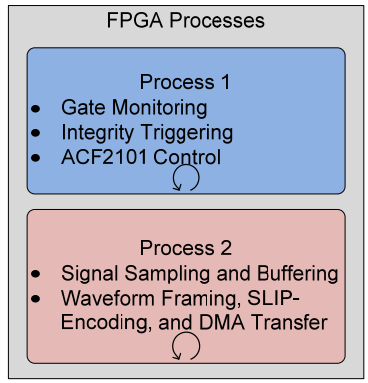

Figure 4: The compactRIO FPGA program architecture.

acquire a set amount (typically 8) of post-gate, rising-edge samples across all 34-channels. These samples are temporarily stored in block memory until all samples have been obtained. Once all prescribed samples have been stored in block memory, their data is framed via SLIP (Serial Line Internet Protocol) encoding, a SLIP-encoded trailer frame is appended, and the data is transferred to the DMA (Direct Memory Access) buffer for retrieval by the compactRIO's Real-Time (RT) computer. Data transferred to the RT process consists of 34, 10-sample arrays representing all waveform data obtained from all sense wires from one, 300 ns beam pulse. Since the waveform data generally represents a monotonic function due to the charge integration process, the final values of the waveforms represent the total accumulated charge for those channels and therefore are used to compose the transverse profile of interest.

Integrity Process

The integrity process operates in a similar manner as that of the beam data acquisition process. Subtle differences include the manner in which the integrity process is triggered and how the integrity data is differentiated from beam data as it is transferred through the DMA channel. Since beam signals are characterized by a 20 Hz pulse rate with a 150 µs-long width, an opportunity for triggering an integrity acquisition presents itself within the remaining ~49 ms of dead signal time. Process 1, mentioned previously in the beam data acquisition process, derives a virtual gate signal for process 2 by calculating the period of the last beam gate cycle, and then adding half of that period to the time the next beam gate is expected to occur. This permits the integrity process to be interleaved with the gate signalling, resulting in an interference-free analysis of wire continuity.

RT Software Architecture

The compactRIO RT computer utilizes a low-priority process for EPICS client interaction and a real-time (RT) process for deterministically extracting waveforms from the DMA channel as shown in Fig. 5. The data stream extracted from the DMA channel is reframed and SLIP-decoded for transfer to an appropriate analysis routine. In this way beam data is averaged and presented to EPICS

ISBN 978-3-95450-176-2

variables for operator display while integrity waveforms are compared with threshold values for wire continuity checking.

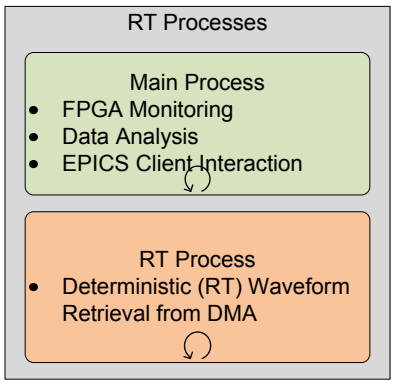

Figure 5: The compactRIO RT program architecture.

SYSTEM PERFORMANCE

Raw beam profiles obtained by the 1L harp system are represented by the red lines in Figs 6 and 7 for the horizontal and vertical planes, respectively. The horizontal profile data indicates a peak intensity level of 3.9 volts, and a standard deviation of 11.48 mm. The vertical profile suffers from a damaged wire at the -12 mm position, causing the Gaussian fit to report an inaccurate standard deviation. From the data it is evident that the particle beam has an elliptical profile with the horizontal axis having the most focused transverse profile and is thus the best profile to compare with the model. Comparing this peak intensity level to the model-predicted level of 4.84 volts indicates a model error of about 19.4%.

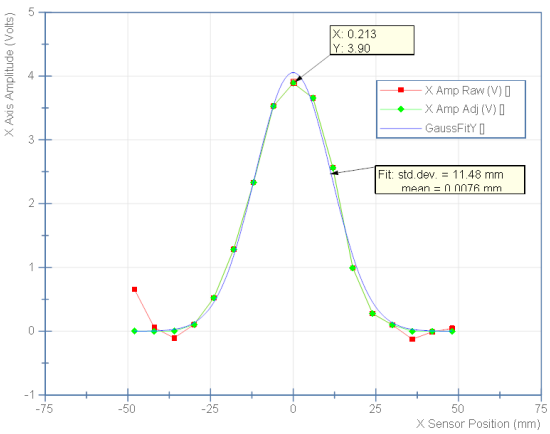

Figure 6: Horizontal profile.

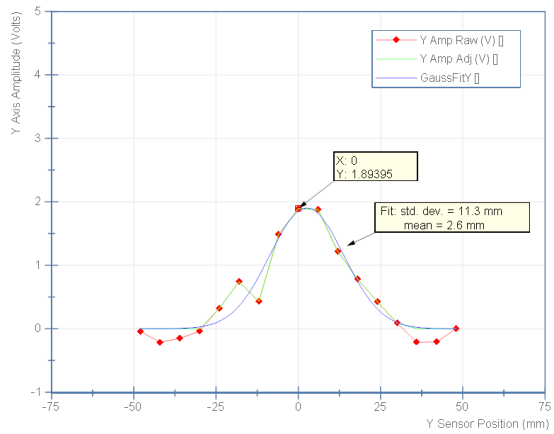

Figure 7: Vertical profile.

CONCLUSION

The model utilized yields a sufficient result for approximating the 1L harp system's electrical exposure to the beam-induced, secondary electron emission and has allowed for predicted signal levels that remain within the system's dynamic range. As for the data acquisition system itself, the compactRIO-based controller and its associated electronics have proven to be a suitable EPICS IOC for obtaining transverse profile measurements from harp diagnostic sensors.

REFERENCES

[1] J.D. Gilpatrick et al.,"LANSCE Harp Upgrade: Analysis, Design, Fabrication, and Installation," TUPSM014, BIW'10, Santa Fe, May 2010: http://www.JACoW.org

[2] W.D. Loveland et al. *Modern Nuclear Chemistry*, (Hoboken: John Wiley & Sons, 2006), 502.

[3] Y. Zhang, et al., "Electronic Stopping Powers in Silicon Carbide," Physical Review B 69, 205201 (2004).

[4] M. Plum, "Interceptive Beam Diagnostics – Signal Creation and Materials Interactions," CP732, BIW '04, Knoxville, May 2004: http://www.JACoW.org

[5] B. Van Zeghbroeck, "Principles of Semiconductor Devices," http://ecee.colorado.edu/~bart/book/gaussian.htm

[6] ACF2101 Data Sheet. www.ti.com/product/acf2101

ISBN 978-3-95450-176-2